Current Applied Science and Technology e-ISSN: 2586-9396

Curr. Appl. Sci. Technol. 2025, Vol. 25 (No. 5), e0263961

Research article

Effect of Discharge Electrode Material on Dust Collection for Electrostatic Precipitator Efficiency

Kewalee Nilgumhang[1], Sarofee Sulaiman[2], Kitısak Komnoi[3], Dusit Ngamrungroj[4], Suebsak Suksaengpanomrung[1] and Wilasinee Kingkam[2]*

[1]Nuclear Fusion and Plasma Section (NFPS), Thailand Institute of Nuclear Technology (Public Organization), Ongkharak, Nakhon Nayok 26120, Thailand
[2]Nuclear Technology Research and Development Center, Thailand Institute of Nuclear Technology, Nakhon Nayok, 26120, Thailand
[3]Advanced Engineering and Nuclear Technology Center (AEN-TeC), Thailand Institute of Nuclear Technology (Public Organization), Ongkharak, Nakhon Nayok 26120, Thailand
[4]Department of Social and Applied science, College of Industrial Technology, King Mongkut's of University Technology North, Bangkok, 10820, Thailand

Received: 10 July 2024, Revised: 16 December 2024 , Accepted: 24 December 2024, Published: 27 March 2025

Abstract

In this study, an electrostatic precipitator collection system for smoke removal from burning incense was developed and the particle collection efficiency was evaluated. The effects of the geometric parameters of a discharge electrode on the dust collection efficiency of the electrostatic precipitator were analyzed, and different types of discharge emission electrodes were optimized. The designed dust collector consisted of a simple array of coaxial discharge electrodes placed along the axis of four cylindrical collection tubes with a diameter of 28 mm with 100 mm in length. The discharging electrodes were of various types: tungsten rods, copper rods and copper wires. DC high voltage power supply was varied with output voltage ranging from 3-10 kV. The distance between discharge electrode and collecting electrode was fixed at 12.5 mm. The air ventilation used in the system had an output velocity of 1.4 m/s, while the collection electrode was grounded. The morphology of the incense ash was studied using scanning electron microscopy (SEM). The experimental results showed that the operational conditions for the ESP were set at a high voltage of 10 kV and a low air flow rate. These conditions, in combination with a tungsten rod as the discharge electrode, provided the highest collection efficiency of PM 2.5 and 10 dust. The overall collection efficiency of the developed precipitator was found to be about 79.51% and 75.68% for PM 2.5 and PM 10. It was shown that the developed prototype was effective in the removal of particulates up to 84.1 and 81.76 for PM 2.5 and PM 10 at the treatment time of 30 min. In conclusion, the developed electrostatic precipitator has the potential as a device for collecting PM 2.5 and PM 10 particles emitted by incense smoke exhaust.

Keywords: electrostatic precipitator; dust collector; discharge electrode; collection efficiency

*Corresponding author: E-mail: wilasinee@tint.or.th
https://doi.org/10.55003/cast.2025.263961

1. Introduction

One of the basic human needs to survive and enjoy life is good weather. However, the weather has changed due to pollution, affecting many people in various countries. Air pollution refers to the contamination of both indoor and outdoor air by gases and solid particles, resulting in changes to the natural characteristics of the air (Maduna & Tomašić, 2017; Manisalidis et al., 2020). Moreover, this contamination can significantly alter the atmosphere's composition, affecting human health, environmental quality, and the global climate. In Thailand, the sources of air pollution include transportation, agricultural burning, industrial activities, residential burning, and others (Vichit-Vadakan & Vajanapoom, 2011). Key pollutants that pose significant health risks include particulate matter (PM), nitrogen oxides (NO_x), sulfur dioxide (SO_2), carbon monoxide (CO), volatile organic compounds (VOC_s), among others (Zukeran et al., 1999). These air pollutants are often invisible to the naked eye because the particles involved are too small for the human eyes to see. However, in certain situations, air pollution can become visible. Household air pollution is an established determinant of human health. World Health Organization (2024) estimates that household air pollution causes around 4.3 million deaths worldwide annually. The preponderance of these fatalities transpires in low- and middle-income nations, especially in Asia, where solid fuels like biomass and coal are often used for cooking and heating.

The current research has determined that the primary cause of air pollution in households is the burning of solid fuel (Ali et al., 2021). Other sources of indoor air pollution include smoking and home cleaning. Nevertheless, the impact of burning incense in residential homes within communities has been largely overlooked in the existing literature. Incense has been utilized for spiritual, magical, cleansing, and healing purposes since ancient times (Jetter et al., 2002; See & Balasubramanian, 2011). Incense burning is widespread in Eastern cultures and religions, particularly in Southeast Asia. Incenses are burned at homes and in public places including places of worship, stores and shopping malls. Various incense forms include sticks, joss sticks, cones, coils, powders, rope, or smudge bundles (Chen et al., 2017). Incenses are usually made from aromatic ingredients, wood powder, adhesive, and bamboo sticks (Lin et al., 2008). Burning incense produces fine and ultrafine particulate matter, volatile organic compounds, other gaseous compounds, and heavy metals (Yang et al., 2006; 2012).

Among those pollutants, particulate matter emitted from incense burning, especially fine PM2.5 and PM10 is one of the most hazardous air pollutants associated with major mortality cases globally (Gupta et al., 2023). Various techniques can be employed to control the dispersion of dust and smoke particles that result from incense burning, including the utilization of high-efficiency particulate air (HEPA) filters and electrostatic precipitators (Dubey et al., 2021). Air filters provide the maximum level of efficiency in filtration, but their use is hindered by challenges in maintenance and the reduction of hot gas pressure. reduction of hot gas pressure. Various techniques can be used to control the dispersion of dust and smoke particles generated from incense burning, including high-efficiency particulate air (HEPA) filters and electrostatic precipitators (Dubey et al., 2021). While HEPA filters offer high filtration efficiency, their use is limited by maintenance challenges and a reduction in airflow pressure. Additionally, elevated temperatures may affect filter performance and durability. Since incense smoke can reach high temperatures, some filtration methods may become less effective or unsuitable. Therefore, alternative approaches, such as electrostatic precipitators or specialized filtration systems, may be more appropriate for capturing fine particles from incense smoke. Using electrostatic precipitator (ESP) air cleaners is effective in reducing industrial and

indoor air pollution, with a 99% efficiency for suspended particulate removal (Hensel et al., 2003; Liu et al., 2022). ESP air cleaners first charge suspended particulates using high-voltage discharge, and then collected by dust collection plates. The collection rate increases with discharge voltage, and the surrounding air can form a plasma, destroying gaseous air pollutants (Liu et al., 2022). The maximum load during the operation of the ESP is assessed using electrodes; hence, the electrode material must possess excellent electrical and thermal conductivity, along with a high melting point. Tungsten, molybdenum, zirconium, hafnium, yttrium, aluminum, copper, iron, and their alloys serve as electrode materials. The selection of discharge electrode material is contingent upon the performance, durability and system design requirements (Lagarias, 1960). Tungsten electrodes used in ESP offer exceptional durability, high-temperature resistance, and reliability, making them well-suited for rigorous industrial applications where consistent performance and longevity are essential (Xu et al., 2022). In contrast, copper electrodes provide outstanding electrical conductivity, facilitating efficient energy transfer. This characteristic can lower power consumption in ESPs and enhance the efficiency of particle collection (Lu et al., 2024).

Many studies have confirmed that ESP is highly efficient in removing suspended particulates. However, their potential to remove gaseous pollutants and aerosols has not been well researched. This research aimed to study and develop an electrostatic precipitator collection system for smoke removal from burning incense and evaluate its particle collection efficiency. The electrostatic precipitator's dust collection efficiency was investigated according to the discharge electrode material characteristics, and the discharge electrode's shape was optimized. Following that, an experiment was conducted to evaluate the effect of optimizing the discharge electrode on the dust-collecting efficiency of the electrostatic precipitator. The level of improvement resulting from the optimization was then validated.

The electrostatic precipitator (ESP) is a device designed to control air pollution. It utilizes electricity within its system to efficiently separate particles from the air. A simple schematic of an ESP system is depicted in Figure 1. The ESP consists of two types of electrodes. The discharge electrode, the negative pole, is made from metal rods, wires, or flat plates, while the collection electrode is constructed from metal sheet plates or tubes (Afshari et al., 2020). The operational principle of the ESP involves using airflow in conjunction with electrodes to charge the particles. Subsequently, electrostatic forces induce the movement of these charged particles towards the collection electrode, which possesses a pole differing from that of the particles, facilitating their collection on its surface.

The primary categories of ESPs include plate, cylinder, and wet precipitators. During the preliminary phase, particle charging transpires through the application of high voltage to air molecules, resulting in ionization and the production of positive ions and free electrons (Mizuno et al., 2000). The free electrons are drawn to the electrode, whilst the positive ions persist in the air, producing a discernible bright blue or purple luminescence referred to as the corona. Upon entering the electric field, particles collide with positively charged air molecules, thereby acquiring a positive charge. The charged particles are then affected by the electric field, prompting their migration towards the negatively charged collecting electrode, where they accumulate and precipitate. However, at high voltages, particle re-entrainment may occur, affecting collection efficiency.

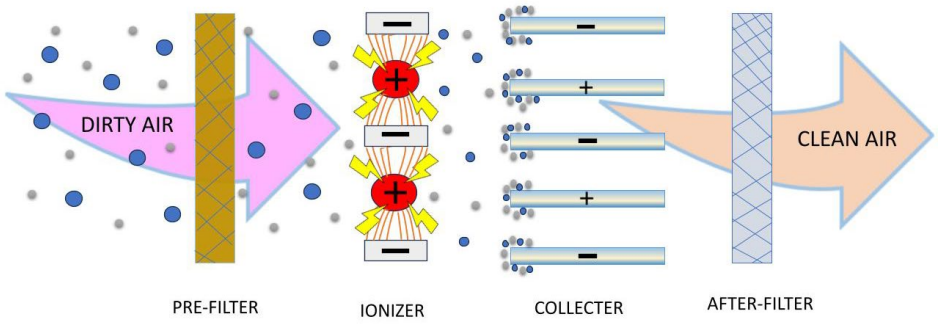

Figure 1. Electrostatic precipitation

Electrostatic precipitators are categorized based on the number of stages employed to charge and eliminate particles from a gas stream. The corona wires are located in the precipitation section in a single-stage precipitator. The electric field responsible for particle charging also induces particle collection on surfaces with an opposing charge within the same chamber (Kocik et al., 2005)

Alternatively, two-stage electrostatic precipitators consist of distinct compartments for the processes of charging and collection. In the first stage, particles are charged using low voltage, while in the second stage, these charged particles are gathered by surfaces that carry an opposite charge. The main purpose of a two-stage ESP is to purify air in combination with IAQ systems. It also helps regulate fine mists and particles in industries such as manufacturing, healthcare, and electronics (Afshari et al., 2020).

A corona discharge is an electrical discharge caused by the ionization of a fluid, such as air, surrounding a high-voltage conductor. It represents a local region where the air (or other fluid) has undergone an electrical breakdown and become conductive, allowing charge to continuously leak off the conductor into the air. A corona discharge occurs at locations where the strength of the electric field (potential gradient) around a conductor exceeds the dielectric strength of the air. Electric field strength E(r) at any radial distance can be calculated using the following equation (Kudpa et al., 2016):

$$E(r) = \frac{V}{r\ln(r_1 / r_2)} \quad (1)$$

Where E(r) is the electric field intensity, r_2 is the radius of the collecting electrode, r_1 is the radius of the discharge electrode, and V is voltage. A corona onset field strength can be calculated as follows (Parker, 1997):

$$E_0 = E_s(\delta + A\sqrt{\delta / r_1}) \quad (2)$$

Where Es is the breakdown electric field in the air at normal conditions (3.126 ×106 V/m for atmospheric pressure of 20°C), A is a constant (0.0266 m1/2), and δ is air density at atmospheric pressure. If the precipitator is a coaxial cylinder and the space charge effect is not taken into account, the corona initiation voltage V_0 can be calculated from the following equation (Parker, 1997).

$$V_0 = Er_1 \ln (r_1 / r_2) \quad (3)$$

The current flowing through the surface area of the outer electrode as a function of the discharge electrode supply voltage can be written as follows (Parker, 1997).

$$I = \frac{8\pi\varepsilon_0 Z_i V(V - V_0)}{r_2^2 \ln(r_2 / r_1)} \quad (4)$$

where ε_0 is the Free-space permittivity, equal to 8.854 x10^{-12} F/m, and Z_i is the electrical mobility of ions and has a value equal to 1.15 x 10^{-4} m^2/v.s. Collection efficiency (η) of the electrostatic precipitator is the proportion of the difference between the masses of the particles at the inlet and outlet of the precipitate to the mass of particles at the inlet of the precipitate (Intra et al., 2010):

$$\eta = 1 - \exp\left(-\frac{wA}{Q}\right) \quad (5)$$

where A is the collection area of the plates of ESP, w is migration velocity, Q is the flowing rate of the gas stream, m_1 is the inlet dust concentration, and m_2 is outlet dust concentration.

2. Materials and Methods

2.1 Materials

The incense used in this study was acquired from a Thail local market. The incense ash was removed and collected from the air using high-voltage electrostatics. The chemical element of the incense was identified using wavelength dispersive X-ray fluorescence (WD-XRF, Bruker S8 Tiger, Germany). The incense ash's morphology and particle size were analyzed using a field emission scanning electron microscope (Hitachi, high-vacuum FE-SEM SU5000). In this work, tungsten-based electrode (with 2 wt.% ThO_2) materials were compared to copper-based alloys (rod and wire type).

2.2 Experimental setup

To evaluate the effectiveness of electrostatic precipitators (ESP) for air treatment applications, a wire-to-cylinder type ESP has been designed and developed, as shown in Figure 2. A laboratory scale ESP consisted of a vertical grounded metal cylinder of inner diameter (D) of 28 mm and length (L) of 100 mm as a collecting electrode. Figure 3 shows the schematic of an ESP section. The ESP section was of the wire-to-cylinder configuration. A copper pipe was used as the collection electrode. Discharge electrodes of different materials types including tungsten rod, copper rod, and copper wire were used and connected to a negative DC high-voltage power supply. The performance of ESP was studied at various voltages ranging from 3 to 10 kV. The system included a 1.4 m/s velocity air output ventilation. A particle counter (HT-9600) was placed to measure the amount of particles. The current and voltage were tested by oscilloscope (tektronix 3 series mdo) to check the accuracy of the voltage. This study used particulate matter (PM 2.5 and PM 10) as the incense smoke markers.

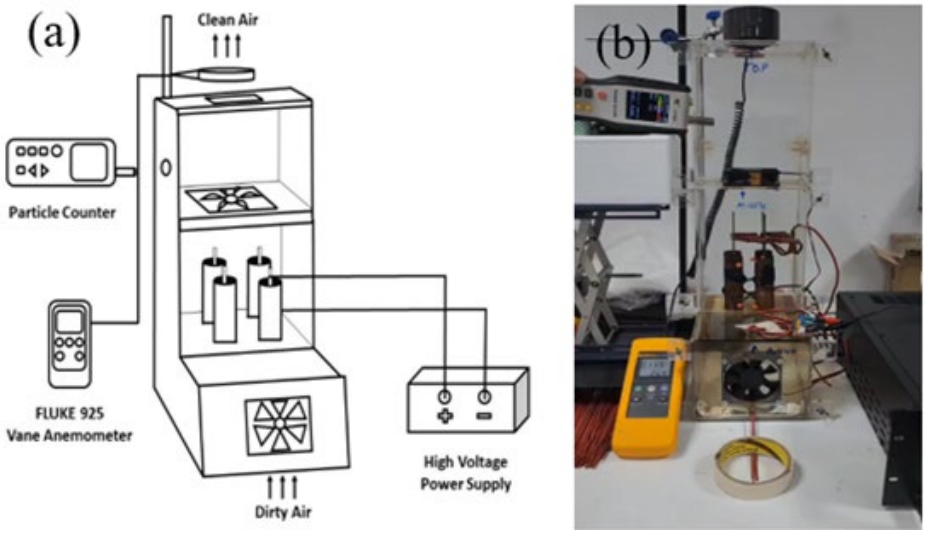

Figure 2. (a) Schematic design of ESP and (b) ESP experimental setup

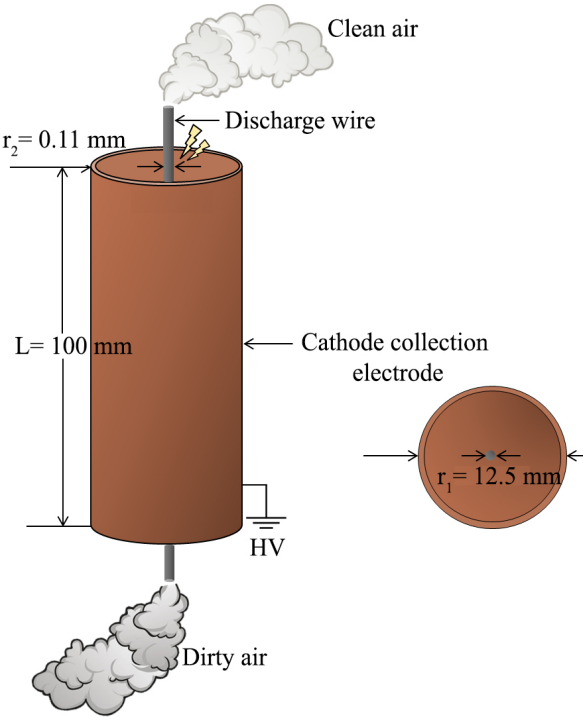

Figure 3. Schematic of an ESP section

The instrument measured the mass concentration of PM 2.5 and PM 10 per minute for 30 min. The collected data was transformed into an average value per minute to align with the desired standard of the instrument. Ten sampling sets were conducted to assess the mass concentration and particle count to determine the percentage of each PM size concentration. The efficiency was determined by analyzing the data collected from the sample observations and comparing it with the percentage of PM size concentration. The impact of temperature was standardized by employing the appropriate formulae for calculating volume under normal conditions. The concentration of PM 2.5 and PM 10 ($\mu g/m^3$) received from the measurement was used to determine instrument efficiency. The efficiency of an air cleaning device can be assessed by directly comparing the ratio of the concentration of dust that had been reduced to the concentration of dust that was initially present (standard approach), and was evaluated as follows (Cid et al., 2022):

$$\eta = 1 - (m_2 / m_1) \quad (6)$$

where m_1 is the inlet dust concentration (g/m^3) and m_2 is the outlet dust concentration (g/m^3). Before the start of each experiment, the particles were discharged by dispersing them onto a copper metal cylinder connected to the ground. Subsequently, the charge was quantified before and after each experiment. In addition, following each experiment, the ESP was dismantled and meticulously cleaned using compressed air. All the experiments were repeated thrice and conducted under stable temperature conditions in the range of 20-25°C and humidity of 40-50%.

3. Results and Discussion

3.1 Dust collector prototype

The dust collector prototype used in this study was developed using current knowledge and electrostatic technology and techniques. Figure 2 depicts the configuration of the newly designed indoor dust collector. The initial prototype was improved based on numerous ideas that met the requirements for utilization in hospitals, buildings, and general offices, and was characterized by being small, light, and easily movable. The improvement was appropriate for utilization inside structures and enclosed spaces. Table 1 presents the chemical composition data for incense ash. The test results show that the ash consisted primarily of $CaCO_3$ (98%), with 2.5% being K_2O and 1.6% being MgO. Table 2 shows the condition variable used to measure the effectiveness of the incense collector from ESP. The prototype consisted of an ionizer, an electrostatic collector, a computer fan, a high-voltage power supply, and an electronic control unit. The prototype first draws air through the machine using an exhaust fan through a coarse filter to filter out coarse dust first. Then, the air flows through into the particle charger.

In this research, we used the diffusion and field charging method to charge dust particles with a positive electric charge. The particle charger consisted of a discharge wire-to-cylinder where the voltage supplied to the discharge electrode was a direct current voltage higher than the corona onset voltage and did not exceed spark-over corona voltage. The voltage polarity was varied from 3-10 kV. A positive pole was used because positive corona voltage creates lower ozone (O_3) than negative corona voltage and was suitable for use inside buildings. Electrically charged particles passed through a particle collector and dust particles were collected using the collecting electrode. A high voltage was provided for the collection and discharge electrodes, releasing clean air from the prototype.

Table 1 X-ray fluorescence analysis of the elemental composition of incense stick ash

Element	Concentration (%)
$CaCO_3$	92.07
K_2O	2.53
SiO_2	1.67
MgO	1.53
P_2O_5	0.54
Cl	0.47
SO_3	0.41
Al_2O_3	0.32
$Fe2O_3$	0.26
TiO_2	0.08
SrO	0.06
MnO	0.03

Table 2. Condition variable used to measure the effectiveness of the incense collector from ESP

Variable	Details
Dimension of prototype	16x22x15 cm (Top) 16x10x44 cm (Bottom)
DC Voltage	3, 7, 10 kV
Corona discharge	rod, wire
Discharge electrode diameter	28.4 mm
collection electrode diameter	wire 0.8 mm rod 1.2 mm
Gap of the discharge and collection electrode	1.2 mm
Velocity	1.4 m/s
Particle charge	PM 2.5/ PM 10
Temperature	30 ^oC
Initial particle concentration	5000 $\mu g/m^3$
Relative humidity	50-70 %RH

3.2 Collecting efficiency

The particle counter measures the proportion of PM 2.5, and PM 10 in the inlet side of the ESP. The collection efficiency (%) of ESP can be evaluated by the inlet concentration or number of particles. Subtract the outlet concentration of particles; the resulting value is divided by the inlet concentration, and all results are multiplied by 100%, as shown in equation 6. Figure 4 shows the incense smoke particle collection efficiencies and dust concentrations for PM 2.5 and PM 10. When the effects of diffusion and gravity sedimentation were combined, the dust particle settling efficiency of the air treatment unit was obtained. It was found that the dust particle collection efficiency value of the ESP increased as the corona discharge and test time increased. A higher voltage directly influenced the electric field strength inside the precipitator, increasing the particle charge. A longer test time allowed the particles to circulate in the prototype for longer, resulting in better precipitation and air treatment. The effects of diffusion and sedimentation influenced by gravity contributed to overall precipitation efficiency. The mean efficiency of the air treatment unit was 79.51% and 75.68% at 30 min for PM 2.5 and PM 10 with a voltage of 10 kV. For PM 2.5, a concentration of incense dust particles at a voltage of 10 kV with tungsten, copper, and copper wire electrode materials had high average efficiencies of 84.1%, 78.48%, and 76.3%, respectively. Followed by 7 kV of all electrodes, efficiencies were 51.38%, 34.98%, and 48.88%. At the voltage of 3 kV, the lowest collection efficiencies were 29.44%, 38.34%, and 39.98 %, respectively. The PM10 concentration test yielded comparable results to the PM 2.5 measurement. The corresponding maximum collection efficiencies at a voltage of 10 kV were 81.76%, 74.28%, and 72.24% for tungsten, copper, and copper wire as the discharge electrodes. However, in the case of PM 10, all electrodes exhibited reduced effectiveness, and certain electrodes had excessively large particle sizes, hence impacting the ESP system and resulting in an undetectable oversized condition. The detector remained efficient, but the ESP system failed to capture these large particles due to insufficient voltage.

Normally, electric field strength is the crucial element that determines the behavior of insulating materials; therefore, analyzing the distribution of electric field strength is essential for the design and sizing of high-voltage equipment. When a high negative DC potential is delivered to the discharge electrode. The grounded collection electrode is elevated, and at a specific voltage, the medium undergoes breakdown, leading to the discharge of free electrons from the discharge electrodes. This occurrence is referred to as “corona discharge”. The most acute electrode is termed the emitter (often a needle or wire), whereas the other is referred to as the collector (plate, ring, mesh, or cylinder) (Chang et al., 1991; Conesa et al., 2019). The common electrode arrangement in corona discharge on ESP also influences collection efficiency through differences in electric field distribution, particle charging, corona discharge, particle transport, and power consumption. The wire-to-cylinder configuration in this study has high importance because it can be used as a source to generate an ionic wind due to the nonuniform electric field created when a high voltage is applied (Kiousis et al., 2014). In contrast, the wire-to-plane arrangement (Carreno & Bernabeu, 1994) has different characteristics. Specifically, the surface condition of the wire such as microscopic roughness and non-uniformity can influence the inception voltage and the corona current discharge. These factors may lead to unstable corona operation in an electrostatic precipitator (ESP) system, affecting its overall performance.

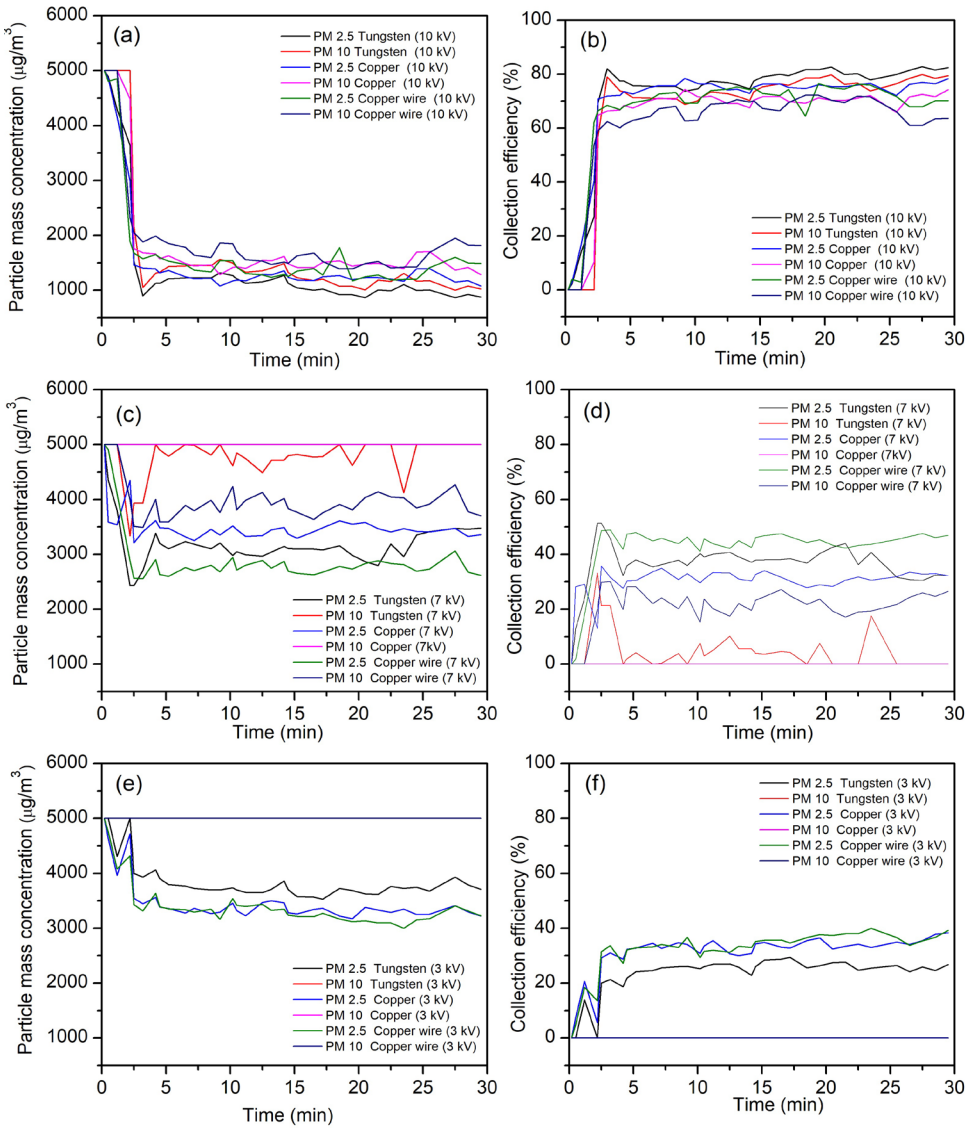

Figure 4. Reduction of total dust concentration and collection efficiency versus time at high voltage (V) values of 3, 7 and 10 kV

In addition to the arrangement of the electrode poles, another factor that affects dust collection efficiency is positive or negative polarization (White et al., 1974). For negative corona (in an experiment), electrons move towards the collecting electrode and positive ions migrate towards the discharge electrode (Wettervik et al., 2015; Park & Chun, 2002). Particle charging takes place in the region between the active zone and the passive surface of the electrode. A substantial quantity of neutral ions, negative ions, and some free electrons migrate towards the passive electrode due to the electric field. The elimination of particles is contingent upon Coulomb's law, being proportional to the strength of the applied electric field and the magnitude of charge attained by the particles. Under

the high-voltage power supply, electric fields induced various electrostatic phenomena, some of which were utilized to charge the incense particles and impart a strong electric field in the smoke to collect and remove them (Riehle, 1997; Nóbrega et al., 2004). Two dust charge mechanisms are possible, contingent upon particle size: field charging for particles approximately 1 μm or bigger, and diffusion charging for particles less than 0.01 (White et al., 1974; Parker, 1997). This study also investigated the effect of PM 2.5 and PM 10 concentrations. Figures 3(a,c,e) show the reduction in PM 2.5 and PM 10 dust levels inside the test machine for 1-30 min. The results show that the amount of PM 2.5, and PM 10 dust in the test chamber decreased when the treatment machine was turned on at voltage of 10 kV for approximately 30 min. The amount of PM 2.5 and PM 10 dust at initial concentrations of 5000 μg/m^3 decreased with increase of voltage. Table 3 shows the results for measuring the efficiency of the dust trap with 5 repetitions under optimum conditions with a tungsten rod electrode with an output voltage of 10 kV.

Table 3. Test results for measuring the efficacy of a dust trap were conducted 5 times

Collection Efficiency (%)	Times						Average
	1	2	3	4	5	6	
PM 2.5	84.1	79.4	81.5	79.52	80.34	72.22	79.51
PM 10	81.76	74.58	78.68	76.22	76.72	66.12	75.68

These results in Table 3 indicate a consistent average collection efficiency of 79.51% and 75.68% for PM 2.5 and PM 10 across all trials. The data suggests that the dust trap effectively captured particles with high accuracy. Comparing the effects of electrode material type on particle collection efficiency, for the same voltage, the tungsten rod's discharge current and collection efficiency were higher than those of the copper rod and copper wire. This is because tungsten has excellent electrical and thermal properties, as well as a higher melting temperature than copper materials (Hamidi et al., 2021).

Therefore, the tungsten rod generated a stronger electric field and attracted particles more effectively. Additionally, the higher melting temperature of tungsten allowed for more efficient particle collection without compromising the integrity of the electrode material. Kim et al. (2016) reported the effects of various materials used as discharge electrodes (tungsten) on ozone emission. It was found that a tungsten electrode, when the voltage was applied in the range of 8-10 kV, released more ozone compared to other metal electrodes. Also, releasing lower ozone concentrations from an ionizer with appropriate high-voltage electrodes can capture air pollutants and destroy chemical pathogens (Park et al., 2016; Baggio et al., 2022).

3.3 Materials characterization

The X-ray diffraction (XRD) technique is highly applicable for determining materials' crystal structures, defects, and elemental compositions. Regarding this, we performed the XRD analysis of the raw incense at room temperature in the range of 10-60 2θ degrees. Here, the lower-degree angle identified organic material contents along with some alkali metals.

Figure 5 displays the XRD patterns of the incense ash. The sample exhibited diffraction peaks at 2θ angles of 23.06, 29.4, 31.43, 35.98, 39.42, 43.12, 47.50, 48.51, and 58.08. The XRD patterns confirmed the existence of calcite, a crystalline manifestation of calcium carbonate, as the main phase of incense (Jain et al., 2020). These XRD results were consistent with the XRF results that found that the concentration of incense ash was

so high that it was not possible to find another mixed compound. This indicates that the incense ash sample was highly pure and did not contain significant impurities.

FESEM-EDX can be used to accurately examine the size, shape, and elemental compositions of materials. Our materials were analyzed using an energy level of 10 KeV to prevent any damage to the materials throughout the analysis process. Upon examination of incense ash using the FESEM, as shown in Figure 6(a). It was clear that the particles exhibited a significant degree of aggregation, resulting in the formation of a cohesive mass. The EDX study (Figure 6(b)) demonstrated the presence of a diverse range of elements inside the incense ash, with calcium (Ca), oxygen (O), and magnesium (Mg) representing the most abundant. Small levels of silicon (Si), carbon (C), and potassium (K) were also identified. The particle size of the raw incense ash powders typically varied within the micron range of 0.9-1.2 microns. Furthermore, the powders of the incense sticks exhibited uneven shapes and sizes, as can be seen in Figures 6(c) and 6(d). The majority of the bright areas consisted of carbon-rich particles, which were generated from the combustion of the stick rising, followed by the elements oxygen (O), potassium (K), and silicon (Si), respectively.

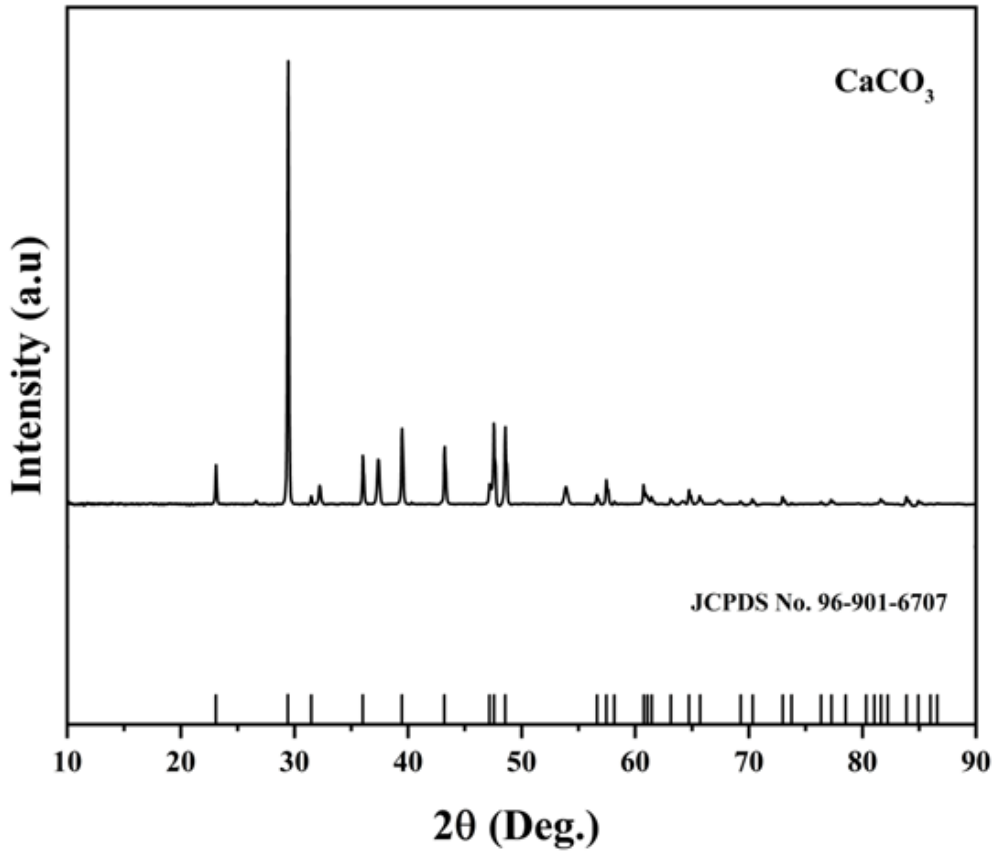

Figure 5. XRD patterns of incense ash

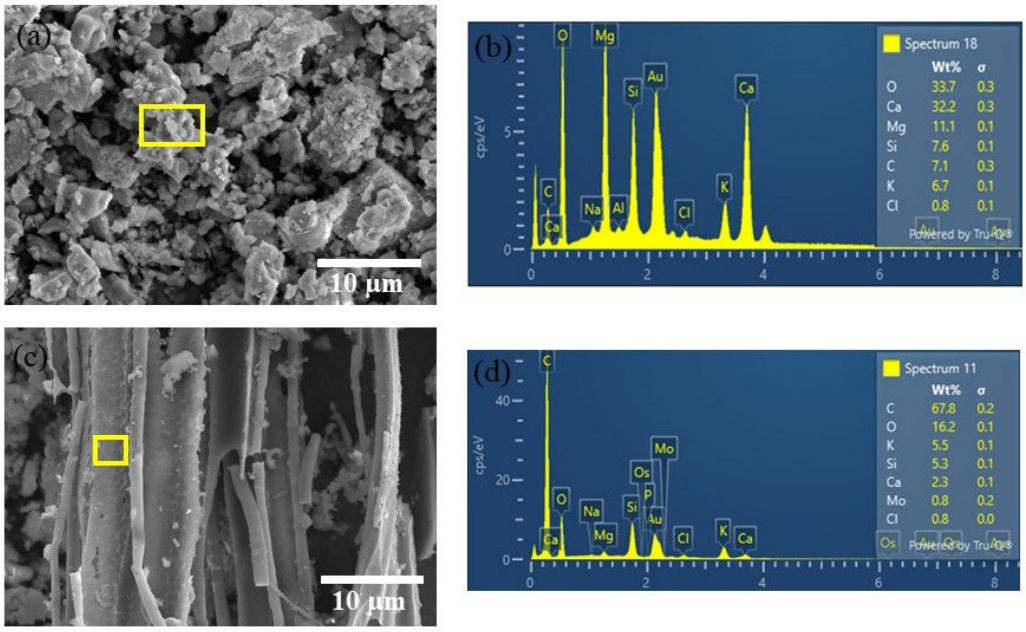

Figure 6. SEM micrographs and EDX spectra of; (a,b) incense ash and (c,d) incense stick ash

4. Conclusions

The experimental results showed that the operational conditions for the ESP were set at a high voltage of 10 kV and a low air flow rate. These conditions combined with the use of a tungsten rod as a discharge electrode provided the highest collection efficiency of PM 2.5 and 10. The overall collection efficiency of the present precipitator was found to be about 79.51 and 75.68% for PM 2.5 and PM 10. It was shown that the developed prototype could effectively remove particulates up to 84.1 and 81.76 for PM 2.5 and PM 10 at the treatment time of 30 min. The effect of electrode materials showed that tungsten rods had higher discharge current and collection efficiency than copper rods and wires due to their superior electrical and thermal properties and higher melting temperature, enabling more effective particle attraction and electrode material integrity. In conclusion, the developed electrostatic precipitator has the potential to collect PM 2.5 and PM 10 particles emitted by incense smoke exhaust.

5. Acknowledgements

The authors acknowledge the financial support of Thailand Science Research and Innovation (contract No. 204542) and Thailand Institute of Nuclear Technology (Public Organization).

6. Conflicts of Interest

The authors declare that they have no conflicts of interest.

References

Afshari, A., Ekberg, L., Forejt, L., Mo, J., Rahimi, S., Siegel, J., Chen, W., Wargocki, P., Zurami, S., & Zhang, J. (2020). Electrostatic precipitators as an indoor air cleaner—a literature review. *Sustainability*, 12(21), Article 8774. https://doi.org/10.3390/su12218774

Ali, M. U., Yu, Y., Yousaf, B., Munir, M. A. M., Ullah, S., Zheng, C., Kuang, X. & Wong, M. H., (2021). Health impacts of indoor air pollution from household solid fuel on children and women. *Journal of Hazardous Materials*, 416, Article 126127. https://doi.org/10.1016/j.jhazmat.2021.126127

Baggio, A., Marino, M., & Maifreni, M. (2022). Effect of negative air ionization technology on microbial reduction of food-related microorganisms. *LWT,* 169, Article 113998. https://doi.org/10.1016/j.lwt.2022.113998

Carreno, F., & Bernabeu, E. (1994). On wire-to-plane positive corona discharge. *Journal of Physics D: Applied Physics*, 27(10), Article 2136. https://doi:10.1088/0022-3727/27/10/022

Chang, J. S., Lawless, P. A., & Yamamoto, T. (1991). Corona discharge processes. *IEEE Transactions on Plasma Science*, 19(6), 1152-1166. https://doi:10.1109/27.125038

Chen, Y. C., Ho, W. C., & Yu, Y. H. (2017). Adolescent lung function associated with incense burning and other environmental exposures at home. *Indoor Air,* 27(4), 746-752. https://doi:10.1111/ina.12355

Cid, N., Patiño, D., Pérez-Orozco, R., & Porteiro, J. (2022). Performance analysis of a small-scale electrostatic precipitator with biomass combustion. *Biomass and Bioenergy,* 162, Article 106500. https://doi.org/10.1016/j.biombioe.2022.106500

Conesa, A. J., Sánchez, M., León, M., & Cabrera, Á. (2019). Some geometrical and electrical aspects on the wire-to-cylinder corona discharge. *Journal of Electrostatics,* 100, Article 103355. https://doi.org/10.1016/j.elstat.2019.103355

Dubey, S., Rohra, H., & Taneja, A. (2021). Assessing effectiveness of air purifiers (HEPA) for controlling indoor particulate pollution. *Heliyon,* 7(9). https://doi:10.1016/j.heliyon.2021.e07976

Gupta, N., Agarwal, A. K., Singhal, R. K., Jindal, S. K., Ali, D., Wanale, S. G., Kumar, G., Yadav, V. K., & Patel, A. (2023). Removal of incense smoke and corollary particulate matter using a portable bipolar air ionizer in an unventilated setup. *Frontiers in Environmental Science*, 11, Article 1218283. https://doi.org/10.3389/fenvs.2023.1218283

Hamidi, A. G., Arabi, H., & Rastegari, S. (2021). The effect of microstructural aspects of WCu composites on electrical conductivity and thermal erosion. *International Journal of Refractory Metals and Hard Materials*, 101, Article 105685. https://doi.org/10.1016/j.ijrmhm.2021.105685

Hensel, K., Pawlat, J., Takashima, K., & Mizuno, A. (2003). Treatment of HCHO using corona discharge and pellet catalysts. In *The 30th International conference on plasma science, 2003. IEEE Conference Record-Abstracts.* (p. 276). IEEE. https://doi.org/10.1109/PLASMA.2003.1228819

Intra, P., Limueadphai, P., & Tippayawong, N. (2010). Particulate emission reduction from biomass burning in small combustion systems with a multiple tubular electrostatic precipitator. *Particulate Science and Technology*, 28(6), 547-565. https://doi.org/10.1080/02726351003758444

Jain, S. N., Tamboli, S. R., Sutar, D. S., Mawal, V. N., Shaikh, A. A., & Prajapati, A. A. (2020). Incense stick ash as a novel and sustainable adsorbent for sequestration of Victoria Blue from aqueous phase. *Sustainable Chemistry and Pharmacy*, 15, Article 100199. https://doi.org/10.1016/j.scp.2019.100199

Jetter, J. J., Guo, Z., McBrian, J. A., & Flynn, M. R. (2002). Characterization of emissions from burning incense. *Science of the Total Environment*, 295(1-3), 51-67. https://doi.org/10.1016/S0048-9697(02)00043-8

Kim, H. J., Han, B., Woo, C. G., & Kim, Y. J. (2016). Ozone emission and electrical characteristics of ionizers with different electrode materials, numbers, and diameters. *IEEE Transactions on Industry Applications*, 53(1), 459-465. https://doi.org/10.1109/TIA.2016.2606362

Kiousis, K. N., Moronis, A. X., & Früh, W. G. (2014). Analysis of the electric field distribution in a wire-cylinder electrode configuration. In N. Mastorakis & V. Mladenov (Eds.). *Computational Problems in Engineering* (pp. 77-92). Springers. https://doi.org/10.1007/978-3-319-03967-1_7

Kocik, M., Dekowski, J., & Mizeraczyk, J. (2005). Particle precipitation efficiency in an electrostatic precipitator. *Journal of Electrostatics*, 63(6-10), 761-766. https://doi.org/10.1016/j.elstat.2005.03.041

Kudpa, C., Uppama, O., Thatui, A., Yodthip, P., Fungom, S., Yawootti, A., & Intra, P. (2016). Analysis of behavior and collection efficiency of particles in two-stage electrostatic precipitators for particulate matter removal from coffee roasting process. *Journal of KMUTNB*, 26(3), 359-374.

Lagarias, J. S. (1960). Discharge electrodes and electrostatic precipitators. *Journal of the Air Pollution Control Association*, 10(4), 271-274.

Lin, T.-C., Krishnaswamy, G., & Chi, D. S. (2008). Incense smoke: clinical, structural and molecular effects on airway disease. *Clinical and Molecular Allergy*, 6, Article 3. https://doi.org/10.1186/1476-7961-6-3

Liu, C. Y., Tseng, C. H., & Wang, K. F. (2022). The Assessment of Indoor Formaldehyde and Bioaerosol Removal by Using Negative Discharge Electrostatic Air Cleaners. *International Journal of Environmental Research and Public Health*, *19*(12), 7209. https://doi.org/10.3390/ijerph19127209

Lu, J., Jiang, H., Guo, P., Li, J., Zhu, H., Fan, X., Huang, L., Sun, J., & Wang, Y. (2024). Application of copper–sulfur compound electrode materials in supercapacitors. *Molecules*, 29(5), Article 977. https://doi.org/10.3390/molecules29050977

Maduna, K. & Tomašić, V. (2017). Air pollution engineering. *Physical Sciences Reviews*, 2(12), Article 20160122. https://doi.org/10.1515/psr-2016-0122

Manisalidis, I., Stavropoulou, E., Stavropoulos, A., & Bezirtzoglou, E. (2020). Environmental and health impacts of air pollution: a review. *Frontiers in Public Health*, 8, Article 14. https://doi.org/10.3389/fpubh.2020.00014

Mizuno, A. (2000). Electrostatic precipitation. *IEEE Transactions on Dielectrics and Electrical Insulation*, 7(5), 615-624. https://doi.org/10.1109/94.879357

Nóbrega, S. W., Falaguasta, M. C. R., & Coury, J. R. (2004). A study of a wire-plate eletrostatic precipitator operating in the removal of polydispersed particles. *Brazilian Journal of Chemical Engineering*, 21, 275-284. https://doi.org/10.1590/S0104-66322004000200018

Park, J. H., & Chun, C. H. (2002). An improved modelling for prediction of grade efficiency of electrostatic precipitators with negative corona. *Journal of Aerosol Science*, 33(4), 673-694. https://doi.org/10.1016/S0021-8502(01)00205-1

Park, J.-S., Sung, B.-J., Yoon, K.-S., & Jeong, C.-S. (2016). The bactericidal effect of an ionizer under low concentration of ozone. *BMC Microbiology*, 16, Article 173. https://doi.org/10.1186/s12866-016-0785-5

Parker, K. R. (1997). Why an electrostatic precipitator? In K. R. Parker (Ed.). *Applied electrostatic precipitation* (pp. 1-10). Springer. https://doi.org/10.1007/978-94-009-1553-4_1

Riehle, C. (1997). Electrostatic precipitation. In J. P. K. Seville (Ed.). *Gas cleaning in demanding applications* (pp. 193-228). Springer. https://doi.org/10.1007/978-94-009-1451-3_10

See, S. W., & Balasubramanian, R. (2011). Characterization of fine particle emissions from incense burning. *Building and Environment*, 46(5), 1074-1080. https://doi.org/10.1016/j.buildenv.2010.11.006

Vichit-Vadakan, N., & Vajanapoom, N. (2011). Health impact from air pollution in Thailand: current and future challenges. *Environmental health perspectives*, 119(5), A197-A198. https://doi.org/10.1289/ehp.1103728

Wettervik, B., Johnson, T., Jakobsson, S., Mark, A., & Edelvik, F. (2015). A domain decomposition method for three species modeling of multi-electrode negative corona discharge–With applications to electrostatic precipitators. *Journal of Electrostatics*, 77, 139-146. https://doi.org/10.1016/j.elstat.2015.08.004

White, H. J. (1974). Resistivity problems in electrostatic precipitation. *Journal of the Air Pollution Control Association*, 24(4), 313-338. https://doi.org/10.1080/00022470.1974.10469923

World Health Organization. (2024). *Household air pollution*. https://www.who.int/news-room/fact-sheets/detail/household-air-pollution-and-health

Xu, J., Chen, P., Gu, Z., Xi, J., & Cai, J. (2022). Performances of a new type high-temperature tubular electrostatic precipitator with rare-earth tungsten cathode. *Separation and Purification Technology*, 280, Article 119820. https://doi.org/10.1016/j.seppur.2021.119820

Yang, T. T., Lin, S. T., Lin, T. S., & Hong, W. L. (2012). Characterization of polycyclic aromatic hydrocarbon emissions in the particulate phase from burning incenses with various atomic hydrogen/carbon ratios. *Science of the Total Environment*, 414, 335-342. https://doi.org/10.1016/j.scitotenv.2011.11.014

Yang, T. T., Chen, C. C., & Lin, J. M. (2006). Characterization of gas and particle emission from smoldering incenses with various diameters. *Bulletin of Environmental Contamination and Toxicology*, 77(6), 799-806. https://doi.org/10.1007/s00128-006-1214-5

Zukeran, A., Looy, P. C., Chakrabarti, A., Berezin, A. A., Jayaram, S., Cross, J. D., Ito, T., & Chang, J.-S. (1999). Collection efficiency of ultrafine particles by an electrostatic precipitator under DC and pulse operating modes. *IEEE Transactions on Industry Applications*, 35(5), 1184-1191. https://doi.org/10.1109/28.793383